

Imaging of gene expression in living cells and tissues

Robert H. Singer
David S. Lawrence
Ben Ovryn
John Condeelis

Albert Einstein College of Medicine
Department of Anatomy and Structural Biology and
Biochemistry
Biophotonics Center
1300 Morris Park Avenue
Bronx, New York 10461
E-mail: rhsinger@aecom.yu.edu

Abstract. It is possible to observe gene expression within single cells using a tetracycline inducible promoter for activation. Transcription can be observed by using a fluorescent fusion protein to bind nascent RNA. Ultimately, it is desirable to activate a reporter gene within a single cell with only photons. This is achieved by preparing a chemically altered transcription factor that is functionally unable to activate a reporter gene until it is exposed to photon excitation. We apply two-photon imaging to visualize tumor cells expressing a transgene and ultimately this approach will provide the means to activate a specific gene within a single cell within any tissue to ultimately observe its functional significance *in situ*. © 2005 Society of Photo-Optical Instrumentation Engineers. [DOI: 10.1117/1.2103032]

Keywords: noninvasive imaging; gene expression; caged transcription factors.

Paper SS04249R received Dec. 16, 2004; revised manuscript received Apr. 4, 2005; accepted for publication Apr. 5, 2005; published online Oct. 31, 2005.

1 Introduction

It has long been a dream of molecular biologists to study events in living cells in real time. The ultimate version of this dream would be to visualize these events within a living organism so that all the specialized cells could be interrogated for their unique and diverse molecular interactions. Only when this dream becomes a possibility will we really understand the factors controlling such diverse processes as gene expression, intercellular signaling, and cell and tissue remodeling, and ultimately the molecular basis of disease.

How then can we begin to approach this goal technologically? One method is to label genes with reporters so that the process of gene expression can be visualized by the use of fluorescent proteins.¹ In this scenario, the fluorescent protein binds to a specific tag on the RNA that is transcribed from the reporter gene. When the gene is expressed, many nascent RNA transcripts at the site of the gene cause the gene to light up as a bright spot in the nucleus indicating that the gene is "on." Eventually as the gene transcribes more and more RNA molecules at the site of the gene, the completed messenger RNAs (mRNAs) can be seen to leave the site and move out of the nucleus into the cytoplasm, where they make proteins.² If the proteins they make are fused to a fluorescent protein of a different color from the RNA, the protein and the RNA can be seen independently. Furthermore, if the gene itself can be marked with a tag that identifies its location in the nucleus, the gene, the RNA transcribed from this gene, and the protein translated from the RNA can all be observed in the living cell simultaneously.³ This has been accomplished by labeling the DNA with a protein, Lac I that binds to a specific DNA sequence inserted at the site of the gene. The Lac I protein is fused to red fluorescent protein (RFP) so that the gene locus is marked with a red spot in the nucleus. We can also insert a regulatory element that responds to the antibiotic tetracycline

that enables us to turn on this gene at will. When the gene is activated to express RNA, the gene turns green, therefore locating both the red and the green spot coincidentally in the nucleus.⁴ When the RNA translates the protein after traveling to the cytoplasm, it makes a fusion protein that is blue and is targeted to peroxisomes so that it concentrates in discrete structures and is easy to observe. Therefore, these cells represent a model system for living cells that can be induced to display to the microscopist a particular molecular process—gene expression.

Recent developments have made it possible to observe such molecular events in tissue cells of live animals. The two-photon microscope can operate at wavelengths that enable us to visualize multiple fluorescent proteins.⁵ Invasion in breast tumors have been analyzed at subcellular resolution in rat and in mouse adenocarcinoma that grows in a tumor in the mammary fat pad.⁶ Single cells within the tumor tissue can then be observed using an inverted microscope with a high-magnification objective through which the two-photon beam is directed. In principle, the cell reporter system described here can be introduced into tumor cells and tissue culture and those cells in tumors introduced into the animal to form tumor tissue.⁷ The gene could be observed to express when the inducer tetracycline has been fed to the mouse. Ultimately, the reporter system could be introduced into a mouse so that native cells could be observed expressing this particular gene.

What would be ultimately desirable would be to turn on a gene in a cell independent of the other cells surrounding it. In this way, the effect of expressing the gene could be observed in the affected cell compared to unaffected cells around it. This would be a profound way to investigate the effect of specific genes on cells and their neighbors. For instance, if a cancer gene were activated in a cell, how would it affect the cell's behavior and that of the cells around it? We would be able to investigate near-term effects if we know the exact time the gene was activated. Such technology is now within our

Address all correspondence to Robert Singer, Anatomy and Structural Biology, Albert Einstein College of Medicine, 1300 Morris Park Avenue, Bronx, New York 10461. Tel: 718-430-8646. Fax: 718-430-8697. E-mail: rhsinger@aecom.yu.edu

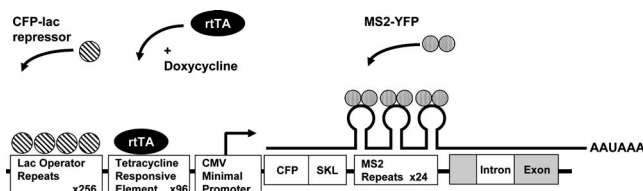


Fig. 1 Construct used to visualize transcription in living cells. The construct contains Lac O repeats to identify the gene, a tet transactivator driving a CMV minimal promoter, a transcription unit coding for CFP with a peroxisome targeting sequence, and 24× MS2 sites in the 3' UTR, followed by a splice site. The Lac O CFP fusion protein binds the Lac O sites and the MS2-YFP binds the MS2 sites on the RNA when the gene is induced by doxycycline. (Adapted from Janicki, et al.³)

grasp—the ability to turn on a specific gene in a specific cell using a beam of light. In this scheme, we have been able to construct an inactive transcription factor with a chemical blocking group that can be cleaved with a particular wavelength of light. Therefore this makes it technically possible to activate a specific gene in a specific cell. This would enable us to activate only those cells that are exposed to the wavelength that we require. If a transgenic mouse contains these components, we would be able to activate a single gene in a single cell anywhere in the animal and then observe the downstream consequences of this intervention. The power of this technique would provide a means to determine the function of any gene anywhere in the animal.

The work presented here details our progress toward achieving this goal of noninvasive activation and monitoring of gene expression.

2 Observing Gene Expression in Living Cells

2.1 Cell Line

A stably transfected cell line was established in which an inducible gene was integrated. The gene contained MS2 stem-loop sequences in the RNA and Lac operator repeat sequences in the DNA. The fusion proteins YFP-MS2 (binds to the stem-loops in the RNA) and CFP-Lac repressor protein (binds to the Lac operator and repeats in the DNA) were driven by the weak L30 ribosomal protein promoter so that the free levels of the fusion proteins in the nucleus were low, to enhance contrast when they are bound to their iterated targets. The YFPs that bind to the 24× MS2 sites and the CFP that binds the DNA repeats were then visible above a homogenous background of unbound fusion protein (Fig. 1).

The reporter gene contains an inducible promoter, “Tet on,” that enables us to turn on the gene at will. The induction enables us to detect the trafficking of RNA from its site of synthesis out of the nucleus. The single integration site provides a focal point for the transcription. Importantly, we have put the Lac repeats into the gene, upstream from the initiation site, so that the gene can be detected independent of the RNA (see Fig. 1). We demonstrated the robustness of the system by inducing the reporter and observing transcription by real-time microscopy (Fig. 2).

2.2 Induction of Transcription and Subsequent Kinetics

The Lac repeats identify the site of the integration. With the activation of transcription, we observe the decondensation of the Lac locus, concomitant with the appearance of the YFP-MS2 binding to the RNA MS2 sites in the nucleus (see Fig. 2). The transcription site increases in intensity as the polymerases load on the gene and begin translocating. After an amount of time consistent with the gene size, individual transcripts are released from the site (Fig. 3). The movement of individual transcripts within the nucleoplasm can be followed with time. We were able to demonstrate that the particles seen in the nucleoplasm in fixed cells contain the amount of signal expected for single RNA molecules, using the identical technology demonstrated in Fusco et al.² (Fig. 4). We then were able to use 2-D imaging in live cells to visualize the movement of these single mRNAs in real time. By tracking pathways of individual nuclear particles we have determined that these RNAs follow a diffusive pattern of movement (Fig. 5). Diffusion coefficients ranged from 0.01 to 0.09 m²/s with average velocities of 0.3 to 0.8 m/s.

3 Light-Initiated Ecdysteroid-Inducible Gene Expression System

Although it is now possible to visually observe gene expression in real time in a living cell, this technology does not provide one with the ability to control where and when transcription occurs. Temporal and spatial control is conceptually possible through the application of light in combination with an appropriately designed photoactivatable (“caged”) molecule that induces gene expression. However, the requirements for the latter molecule are stringent. First, it must influence only the expression of the gene of interest, preferably a transgene, since the insertion of the latter is relatively straightforward. As a corollary, this strategy requires that the small molecule inducer of gene expression have little or no effect on mammalian physiology, to simplify interpretation of the biological consequences of transgene activation. Second, the compound must be cell permeable. Third, the compound must contain a key functional group that, upon covalent modification, results in the loss of biological activity. This key parameter enables one to render the compound inactive using a photosensitive moiety. Upon subsequent exposure to a high-intensity light source, the structure of the original molecule is restored as is its ability to switch on gene expression.

Ecdysone (1), and related ecdysteroids, such as ponasterone A (2) (Fig. 6) are insect molting hormones that have little effect on mammalian physiology. The corpus cardiacum in the insect brain releases a hormone, at various stages of development, that signals the prothoracic gland to produce and release ecdysone. The latter enters cells and induces the formation of a heterodimer between the ecdysone receptor (EcR) and the product of the ultraspiracle gene (USP). The latter complex subsequently binds to the ecdysone response element in the promoter region of targeted genes, which in turn, induces expression and subsequent molting. In 1996, No et al. recognized that this system could be introduced into a mammalian animal model to elicit the expression of any given transgene at any point during the life of the organism.⁹ Albanese et al. subsequently reported an ecdysone-sensitive mouse model as

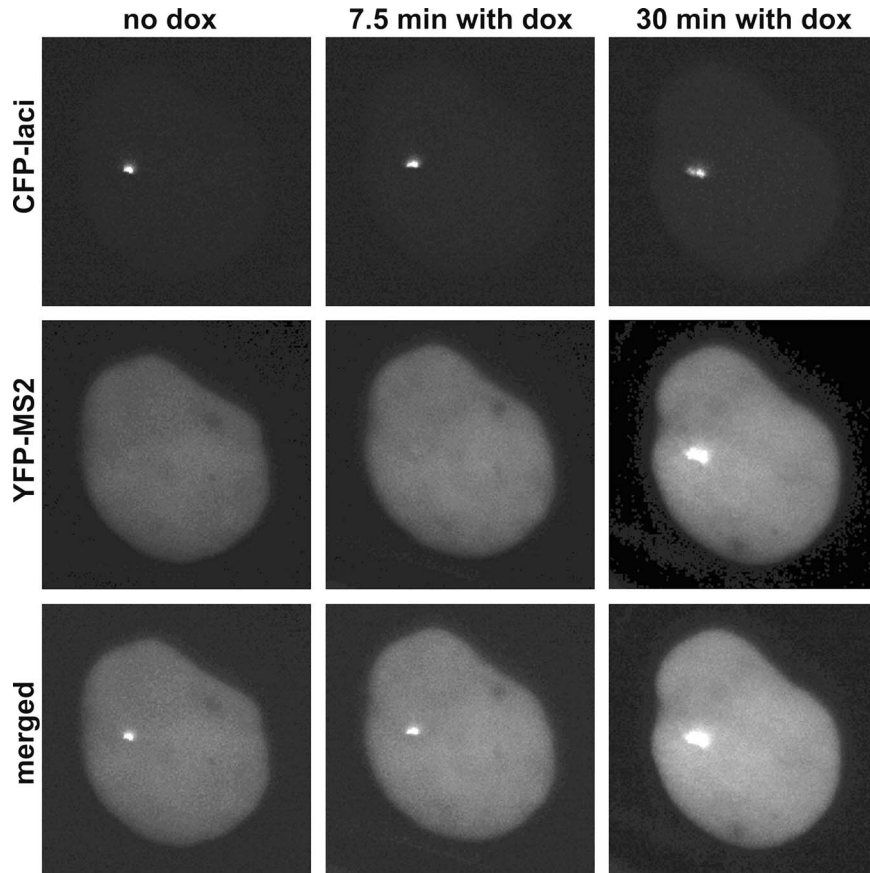


Fig. 2 Induction of gene expression. After a few minutes of exposure to doxycycline, the gene can be seen to decondense (top row), and the RNA synthesis turns on at the transcription site (middle row). Translation of the protein can be seen after 30 min, indicating the RNA is exiting the nucleus and is being translated. (Adapted from Janicki, et al.³)

well.¹⁰ In these constructs, the animal constitutively expresses EcR as well as the mammalian homologue of USP (RXR, retinoid X receptor). The transgene is not expressed until the animal is exposed to ecdysone, or its more potent plant analogue, ponasterone A. The ecdysone-inducible mouse furnishes a solution to the problem of temporal control. However, even with use of tissue-specific promoters, this system is unable to provide fine spatial control in which the expression of a specific transgene is activated in one or a few cells surrounded by otherwise nonexpressing cells. The latter is par-

ticularly important in the onset of certain disease states, such as breast cancer. For example, most breast cancers arise via the oncogenic transformation of epithelial cells that line the mammary ducts followed by clonal expansion. Although tumorigenesis likely proceeds via the transformation of specific

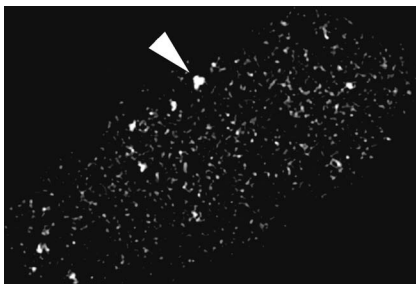


Fig. 3 Single particles of RNA fill the nucleoplasm. The bright transcription site is at the edge of the nucleus. Single RNAs diffuse throughout the nucleoplasm, presumably until they encounter nuclear pores. (Adapted from: Shav-Tal, et al.⁴)

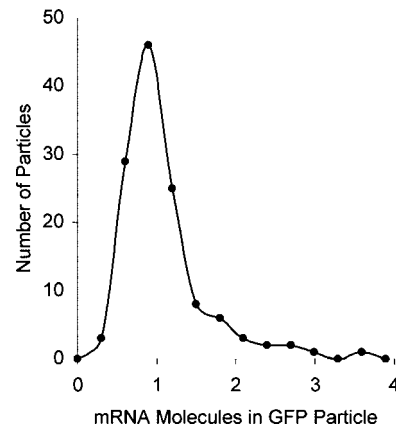


Fig. 4 Particles of GFP in the nucleus are single RNA molecules. Using methods for detecting single molecules in the cytoplasm,^{2,8} quantification of nuclear particles reveals that most particles contain single RNA molecules. (Adapted from Fusco, et al.²).

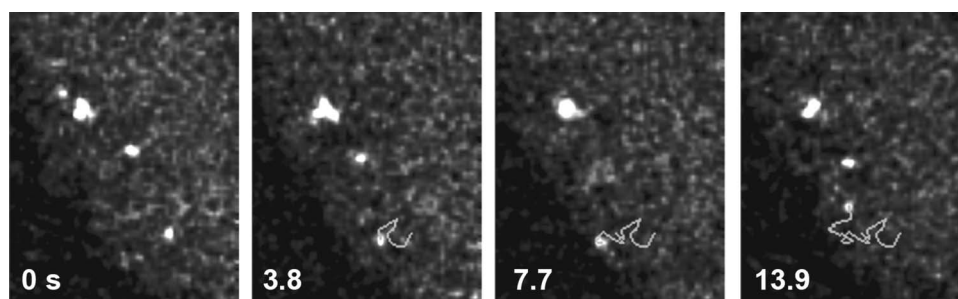


Fig. 5 Particle tracking of single RNA molecules released from the transcription site. An algorithm was designed to follow an RNA molecule through successive frames of the 2-D images with time. This data were then used to show⁴ that the movement fit diffusion equations (mean squared displacement versus time).

individual cell types in anatomically well defined regions, the relative tumorigenic potential of different mammary precursor cells remains a mystery.

In addition to the ecdysone-inducible gene expression system described above, several other strategies have been devised to date, including glucocorticoid-, IPTG-, tetracycline-, and FK1012-dependent systems. However, none of these offer the fine spatial control that is required to explore the relationship between the array of possible precursor cell types and the pathogenesis of breast cancer.¹¹ In more general terms, these inducible gene expression strategies do not enable one to assess the phenotypic consequences of protein expression as a function of tissue microenvironment. One approach to circumvent this limitation is the use of light to control when and where gene activation/protein expression transpires. Cambridge et al. were the first to describe light-induced gene transcription via the preparation of a caged polypeptide transcription factor.¹² Cruz et al. subsequently reported a caged form of estradiol, which was used to drive the expression of an estrogen-response-element-controlled gene.¹³ Given the previously described advantages associated with the ecdysone system,¹¹ we prepared a caged form of ecdysone.¹⁴

The family of naturally occurring ecdysteroids enjoys an illustrious molecular history of several decades of research.^{15,16} A wide variety of semisynthetic derivatives have been prepared and their biological activity surveyed. In general, the free hydroxyl groups in ecdysone are important for biological activity, particularly the hydroxyl moiety at C-2, in Fig. 6, see **1** and **2**^{15,16}. Consequently, it occurred to us that derivatization of this position with a light-sensitive moiety should produce an inactive ecdysone whose activity can be subsequently restored on exposure to high-intensity light. One strategy would be to selectively acylate the C-2 position, thereby producing an ester moiety. However, we were con-

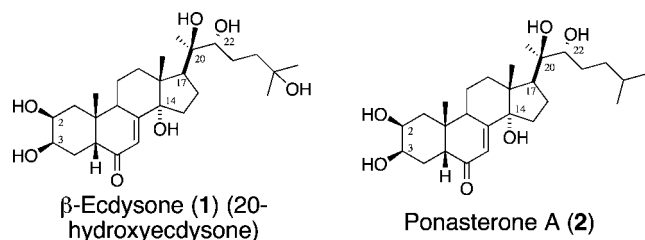


Fig. 6 Ecdysone (**1**) and ponasterone A (**2**).

cerned that the ester moiety might be susceptible to hydrolysis potentially by nonspecific esterases. An alternative approach, namely, alkylation of the C-2 hydroxyl, would furnish a more robust ether moiety. However, although a wide variety of acylated ecdysteroids have been described in the literature, we knew of no example of an alkylated ecdysteroid. Alkylation reactions generally require more vigorous conditions than the corresponding acylations, a potential problem given the known susceptibility of ecdysteroids to dehydration. Indeed, we found that a wide variety of reaction conditions resulted in the formation of various ecdysteroid decomposition products. We ultimately examined an extremely mild method for generating ethers that has been extensively employed in sugar chemistry.¹⁴ The chemistry takes advantage of the presence of the C-2/C-3 diol pair positioned on the A ring of the ecdysteroid (the corresponding vicinal diol at C-20/C-22 is less reactive). The stannylene acetal of **1** (compound **3**) was generated *in situ* and subsequently alkylated with **4** to produce the caged ecdysteroid **5** in 90% yield.¹⁴ Monoalkylation occurred specifically at the desired C-2 position, as assessed by a combination of double-quantum filtered-correlated spectroscopy (DQF-COSY), heteronuclear single-quantum correlation (HSQC), and heteronuclear multiple-bond correlation (HMBC) nuclear magnetic resonance (NMR) spectroscopies. Reassuringly, exposure of **5** to illumination from a Hg arc lamp, using a low-wavelength cutoff filter (<348 nm) and an IR filter, regenerated the uncaged biologi-

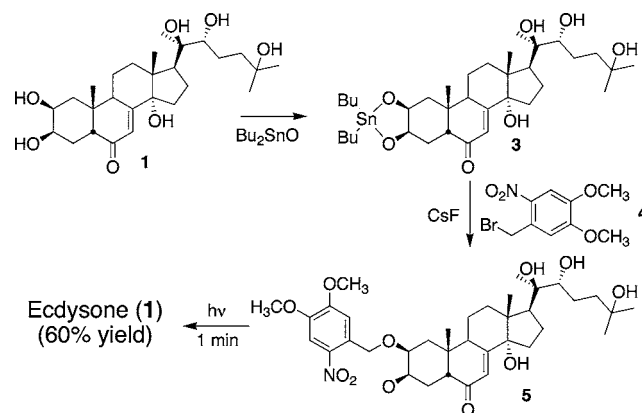


Fig. 7 Preparation of caged ecdysone **5** and its subsequent photolysis to active ecdysteroid.

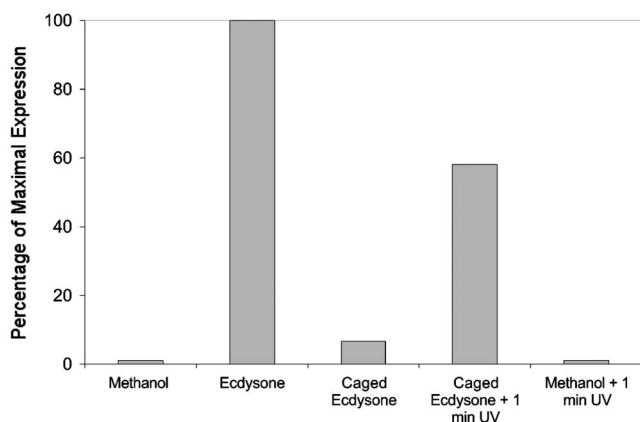


Fig. 8 Luciferase expression in 293T-treated cells transiently transfected with plasmids that code for constitutively expressed EcR/RXR and inducibly expressed (with ecdysone) luciferase. Cells exposed to (a) Buffer alone (containing 2% MeOH), (b) 100- μ M ecdysone (2% MeOH), (c) 100- μ M caged ecdysone (2% MeOH), (d) 100- μ M caged ecdysone (2% MeOH)+1 min $h\nu$, and (e) 2% MeOH +1 min $h\nu$.

cally active ecdysone **1** (60% conversion).

We transiently transfected the 293T cell line with two plasmids.¹⁴ The first codes for constitutively expressed EcR, whereas the second contains a luciferase gene that is coupled to a promoter with an embedded ecdysone response element. The caged ecdysone **5** was added to the transfected 293T cells and the induction of luciferase activity in the presence and absence of light was noted (Fig. 8). Cells exposed to ecdysone **1** display a nearly 100-fold induction of luciferase. As expected, the caged analog **5** is essentially inactive. However, compound **5**, in combination with a 1-min exposure to a high-intensity light source, induces a dramatic enhancement in luciferase production, which is approximately 60% of the expression the bioactive ecdysone **1**. The latter is consistent with our observation that a 1-min photolysis time window converts approximately 60% of the caged derivative **5** into its bioactive counterpart **1**. Finally, photolysis in the absence of the caged ecdysone fails to induce luciferase production. As an aside, ponasterone A is significantly more potent as an inducing agent than ecdysone, generating gene expression levels that are as much as 100-fold higher¹⁰ (i.e., 10,000-fold versus untreated sample). Consequently, we expect the corresponding caged analogue of **2** to exhibit properties that are even more

dramatic than **5**. Furthermore, although relatively long illumination times (several minutes) are often required for photouncaging purposes in large cell populations in culture, light exposure times can be reduced to a few seconds or less when compounds in individual cells are photouncaged under the microscope. The latter is simply a consequence of the high photon flux that is generated under microscopic conditions through a relatively narrow spatial window. Consequently, our expectations are that single cell uncaging *in vivo* using the proper caged ecdysteroid should require only a brief pulse of light to generate a robust response.

The results outlined in Fig. 8 reveal that gene expression can be induced at any time of our choosing. However, additional temporal questions remained, namely, the time dependence of expression. To address the latter, we preincubated the 293T cells with the caged ecdysone **5** for 16 h, photolyzed for 1 min, and subsequently lysed at various time points following photolysis.¹⁴ Maximal gene expression was observed after 16 h. An especially important question concerned whether photouncaging occurs inside cells. If photouncaging transpired only in the extracellular environment, then fine spatial control might be lost. Cells were preincubated with **5** and the media subsequently removed. Following washing of the cells with phosphate buffered saline, an ecdysone-free media was added. Cells were photolysed, incubated to various time points, and tested for luciferase activity. An increase in expression levels as a function of time was observed, which is consistent with the notion that that caged ecdysone **5** is intracellularly liberated.

Although the light-activated ecdysteroid gene expression system has the potential to furnish a more finely tuned temporal control over gene expression than the corresponding standard ecdysteroid system, it is in the area of spatial control that caged transcription factors enjoy the greatest potential. We explored the latter possibility by examining whether the combination of **5** and spot illumination generates spatially discrete gene activation in a multicellular environment¹⁴ (Fig. 9). A series of experiments were conducted to compare and contrast the level of spatial control available with the light-activated system versus its conventional counterpart. The assay simply involved the exposure of transiently transfected 293T cells to ecdysone or its caged counterpart, followed by washing to remove extracellular ecdysteroid. Cells were then either illuminated for 10 s or kept in the dark and then incubated for 16 h. Finally, the cells were fixed, permeabilized, exposed to a luciferase antibody, and stained with an Alexa-

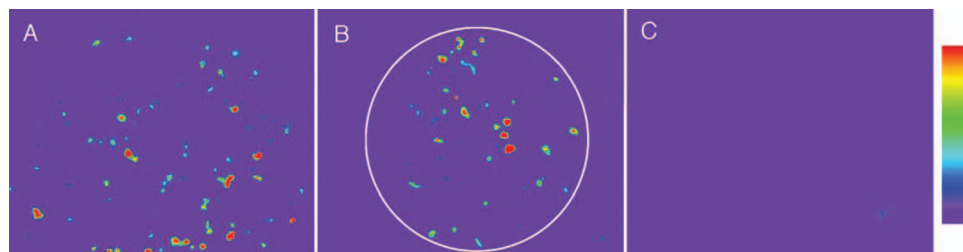


Fig. 9 Activation of the caged ecdysone by light: (A) transfected 293T cells were exposed to ecdysone and subsequently probed for luciferase expression; (B) transfected 293T cells were exposed to **5**, spot illuminated (~ 0.25 mm²) for 10 s, and then probed for luciferase expression; and (C) the experiment as described in (B) outside of the region of illumination. [Olympus IX-70 at 10 \times ; numerical aperture (NA) of 0.3]. (Adapted from Lin, et al.¹⁴)

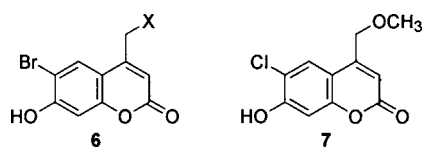


Fig. 10 The coumain-based derivatives **6** (where $X = -O_2CR$, $-O_2P(OR)_2$, or $-O_2CNHR$ are sensitive to photolysis whereas **7** is not.

labeled secondary antibody. Luciferase expression was observed throughout the general cell population on exposure to ecdysone [Fig. 9(A)]. By contrast, cells incubated with the caged analog **5** under identical conditions failed to exhibit detectable luciferase expression. However, luciferase expression was induced in a spatially specific fashion by exposing the entire cell culture to **5**, subsequently replacing the media with fresh media to remove extracellular **5**, and spot illuminating the ($\sim 0.25 \text{ mm}^2$) culture dish. Only those regions exposed to UV light display luciferase production [Figs. 9(B) and 9(C)], which validates the notion that gene expression can be spatially controlled in a multicellular environment.

4 Toward a Two-Photon Sensitive Ecdysteroid System

One of the difficulties associated with the use of one-photon uncaging in whole animals is that illumination with 300- to 400-nm light has poor tissue penetration due to the presence of endogenous absorbing chromophores. Furthermore, conventional photolytic uncaging requires excitation throughout the bulk of the sample. Although both confocal imaging and computer deconvolution can be effective in virtually eliminating out-of-focus light from thick objects, which is necessary for intravital imaging, these techniques do nothing to alleviate another major problem of intravital imaging, excitation of the entire axial volume of irradiation causing excessive uncaging and phototoxicity. Multiphoton technology represents an elegant solution to the difficulties associated with single photon uncaging. Excitation is confined to only the optical section being observed.¹⁷ Under multiphoton conditions, a sample is illuminated at a wavelength approximately twice (or three times) the wavelength normally absorbed by the chromophore.¹⁸ If a chromophore absorbs two (or more) photons within 1 fs, then the energies associated with these photons are combined and absorbed by the chromophore. Consequently, the absorption of two photons of long wavelength is equivalent to the absorption of one photon at half the wavelength. In the case of green fluorescent protein (GFP), which has an absorption peak at approximately 480 nm, 960-nm light can be used for excitation. Essentially no excitation of the fluorophore will occur at the 960-nm wavelength out of the plane of focus because this wavelength is so far removed from the GFP peak excitation wavelength and the photon density is too low for multiphoton excitation. In addition, neither bleaching nor uncaging will occur, nor will phototoxic products be generated in the bulk of the sample. A high-peak-power laser source is used to deliver pulses that are shorter than a picosecond so that the peak-mean-power levels are moderate and do not damage the specimen. One of the clear advantages associated with the use of long-wavelength light is significantly deeper tissue penetration. For example,

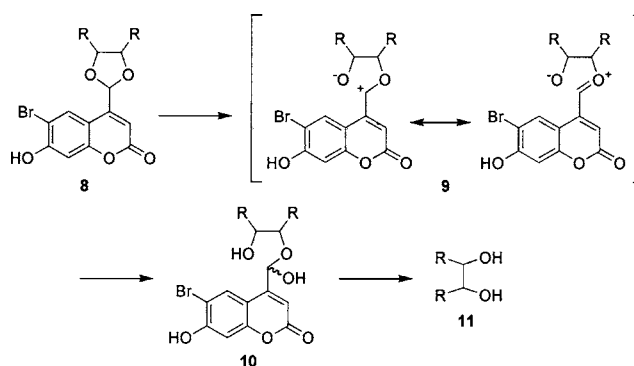


Fig. 11 The coumarin acetal **8** undergoes photo-uncaging via an S_N1 mechanism.

multiphoton-generated cerebral cortex images of live rats were collected at depths of $\sim 0.6 \text{ mm}$ below the surface pia—hundreds of μm deeper than previously imaged using confocal microscopy.¹⁹ With this source, the photon density only at the point of focus will be sufficiently high for significant numbers of two- and three-photon events to occur to generate fluorescence. Similar arguments apply to the use of the multiphoton light path in uncaging that localizes the uncaging reaction to a single optical plane thinner than the dimensions of a single cell.

With the preceding comments in mind, it is clear that the single-photon-sensitive *ortho*-nitrobenzyl moiety used to cage ecdysone (i.e., **5**) is less than suitable for live animal studies. A photolabile-protecting group containing a large two-photon absorbance cross section was recently introduced as a caging agent (**6**) (Fig. 10).²⁰ Although **6** holds significant promise for *in vivo* studies, it has been used to cage only a limited number of functional groups [e.g., carboxylate (**6a**, $X = -O_2CR$), phosphate [**6b**, $X = -O_2P(OR)_2$], and carbamate (**6c**, $X = -O_2CNHR$)]. By contrast, aliphatic alcohols fail to undergo photocleavage when caged with the coumarin moiety (e.g., **7**). Photoliberation likely proceeds via an S_N1 mechanism, which would limit cleavage to functionality that are good leaving groups²¹ (e.g., **6a** to **6c**). We reasoned that it should be possible to promote the photodeprotection of a coumarin-caged aliphatic alcohol if the latter were to lie adjacent to an electron-rich center that could assist the cleavage process. Indeed, we found that aliphatic ethers, when present as a component of 1,2- and 1,4-acetals, undergo light-initiated cleavage.²² A possible mechanism of photocleavage is presented in scheme 2 (Fig. 11). Ecdysone and ponasterone A possess 1,2-diols as well. Consequently, we anticipate that the corresponding acetals of **1** and **2**, respectively, should be sensitive to uncaging by two-photon technology as well. However, unlike the ether linkage in compound **5**, acetals are potentially susceptible to decomposition. This could result in the adventitious formation of active ecdysteroid and thereby generate a high background in the absence of light. Indeed, even simple esters are susceptible to decomposition. For example, an *o*-nitrobenzyl-caged ester derivative of glutamic acid displays a half-life of less than 20 h in the absence of light.²⁰ The corresponding coumarin-caged ester analog of glutamic acid suffers 50% hydrolysis within²⁰ 2 days. By contrast, we are unable to observe any hydrolysis of the 1,2- and 1,4-acetal

ring systems under physiological conditions after 2 weeks. In short, the acetal caging system is hydrolytically inert at neutral pH, bears a large two-photon absorbance cross section, and is applicable to the 1,2-diol structural arrangement present in ecdysteroids.

5 Theoretical Considerations

For two-photon illumination, the number of atoms N uncaged following photoexcitation can be determined from^{23,24}

$$N \propto \frac{\sigma I^2 N_v T}{F \tau},$$

where σ is the two-photon absorption cross section measured; I is the intensity; N_v is the number of caged molecules that are excited by the two-photon illumination; and T is the dwell time of the exciting pulse that is characterized by pulse width τ and delivered with a repetition frequency F . It is useful to obtain an order of magnitude estimate for the release of atoms from a cage that has a relatively large two-photon absorption cross section equal to 1 GM (1 GM, Göppert-Mayer equals 10^{-50} cm⁴ s/photon). Assuming an excitation wavelength of 500 nm focused by a diffraction-limited microscope objective with an NA of 1.4, then the cross-sectional area and axial extent of the beam calculated from the FWHM (full width half maximum) is approximately $A = \pi(0.141 \mu\text{m})^2$ and $0.337 \mu\text{m}$, respectively, yielding²⁵ an excitation volume approximately equal to 2×10^{-17} l (~ 0.02 fl). For a beam intensity of 5 mW at the sample, the intensity becomes $I \sim 2 \times 10^{17}$ photons/(s μm^2). The number of caged molecules excited within this volume is $N_v = C(1 \times 10^7)$ molecules l, where C is the concentration of caged molecules. For a pulsed Ti:sapphire laser, the repetition frequency F and pulse width τ are approximately 80 MHz and 100 fs; with a scanning microscope, the dwell time per pixel might be approximately $T = 20 \mu\text{s}$. Finally, if we assume an intracellular concentration of caged molecules, $C = 100 \mu\text{M}$, then the number of uncaged atoms is of order $N = 12,000$. For a cage with a smaller absorption cross section, for example, 0.01 GM, then the number of atoms would be of the order of 120.

Although these atoms are liberated within the focused beam, they will quickly diffuse from the excitation beam. In addition to the loss of these molecules, caged molecules will diffuse into the region and subsequently become uncaged. It is possible to model this process by solving diffusion-reaction equations.²³

With two-photon excitation, it is possible to limit the photolysis to within the nuclear volume of single cell. For example, Echevarria et al. photolyzed NPE-caged InsP3 within²⁶ the nucleus of SKHep1 cells (1- to 5-mM NPE-caged InsP3 was microinjected into cells with diameter equal to $12 \mu\text{m}$). Using two-photon uncaging combined with confocal imaging, they were able to show significant nuclear Ca^{2+} increase associated with the photorelease of InsP3 in this region of the cell. By contrast, changes in cytosolic Ca^{2+} levels were negligible.

To produce a high concentration of free PonA in the focal volume of the illuminating laser, a series of short pulses must be delivered to photolyze the caged PonA. Following a single pulse of duration δt , the ratio of liberated (uncaged) PonA to

caged PonA will increase as a function of time as $1 - \exp(-Rq\delta t)$, where R is the average photoexcitation rate per molecule (R is proportional to the intensity for one photon excitation and to the intensity squared for two-photons), and q is the quantum yield for the release. Assuming that excitation saturation is negligible, a continuous train of pulses may be used to build up a steady state concentration of free PonA.

Following liberation from the cage, free PonA will diffuse from the focal volume (approximately a femtoliter for two-photon excitation at moderate numerical aperture). The concentration gradient C produced should be analogous to that produced from a pipette that is injecting x molecules/s for a time Δt ($N = x \Delta t$) with a diffusion constant D as given by the following equation:

$$C(r, t) = \frac{N}{(4\pi Dt)^{3/2}} \exp\left(-\frac{r^2}{4Dt}\right).$$

Therefore, the maximum pulse of PonA at a distance r from the center of the focal volume will be delivered at a time $t = r^2/6D$ and is equal to $C = 0.07 N/r^3$. Following this maximum pulse, the concentration decreases as an error function.

Compared with uncaging in the nucleus, where we anticipate very rapid diffusion to the Lac I target, uncaging in the cytoplasm will not have as extremely rapid an effect. Because of the lipophilic nature of steroid hormones, if the uncaging beam is focused in the cytoplasm, free PonA will readily enter the nucleus through the nuclear pores by simple diffusion. Once in the nucleus, PonA will bind²⁷ to form a nuclear heterodimer complex with USP (PonA binds with high affinity $K_D \sim 1$ nM). Although free PonA will diffuse across the nuclear envelope, we assume the nuclear envelope is relatively impermeable to the heterodimer complex. Therefore, it will ultimately associate with the ecdysone responsive element and subsequently drive gene expression.

6 Intravital Imaging: A Comparison of Confocal and Multiphoton Microscopes

We described a method for providing a detailed characterization of the behavior of cells within intact normal tissue and primary tumors in live animals using advanced multiphoton imaging.^{6,28} The method is direct and inherently quantitative, enabling the direct quantification of behavior parameters such as directionality of cell movement toward histological landmarks, velocity and persistence of cell motility *in vivo*, and the motion of particles inside cells *in vivo*. A comparison of the laser scanning confocal microscope with the multiphoton microscope for imaging of primary mammary tumors was done in live anesthetized rats with 2.5-week-old mammary tumors induced by injecting the GFP-expressing cells into the mammary fat pad.²⁹ The nonmetastatic and metastatic tumor cell lines used in these experiments were the MTC and MTLn3 lines, respectively. These cell lines represent a well-characterized cell pair that were derived from the same tumor and that retain their relative metastatic phenotypes after prolonged culture.^{30,31} These cell lines were each prepared to constitutively express GFP. On subcutaneous injection of these cells into the mammary fat pad of female Fischer 344 rats, primary tumors form that fluoresce when excited with 488-nm light, enabling the observation of single cells.⁷

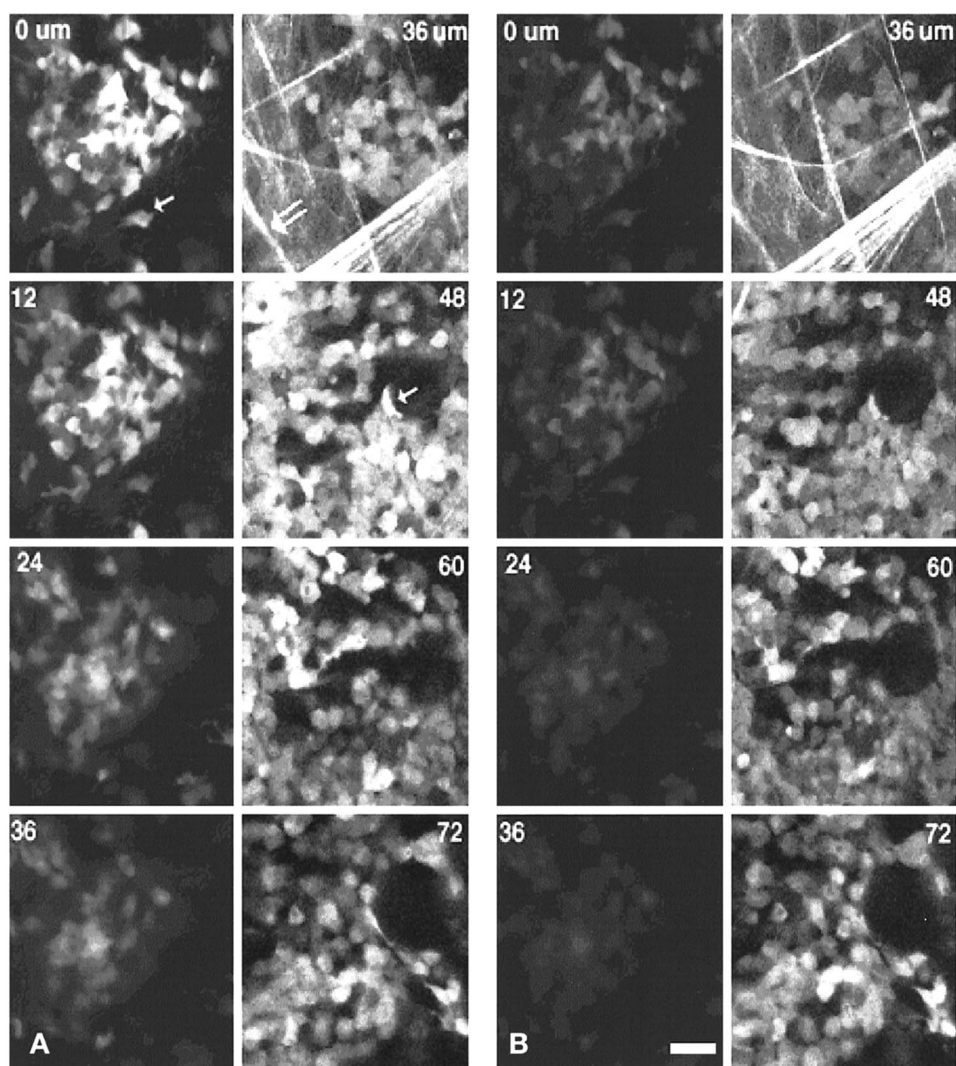


Fig. 12 Comparison of single- and multiphoton microscopy. (A) Depth of imaging in live tumors. Two z series of optical sections at $12\text{-}\mu\text{m}$ intervals (shown in each panel) were obtained with the confocal (left) and multiphoton (right) microscopes. Individual cells are seen as GFP-positive cells (arrows), and collagen and elastin matrix is seen as multiphoton-excited autofluorescent fibers (double arrow), the latter seen in the multiphoton microscope only. (B) Photobleaching in live tumors. A second identical z series of the same field shown in (A) was performed to evaluate the relative bleaching of GFP fluorescence in the live primary tumor. The SNR of the confocal images is unacceptable at all levels, while that of the multiphoton images suffered no perceptible bleaching.²⁹ Magnification bar, $30\ \mu\text{m}$. (Adapted from Wang, et al.²⁸)

In both imaging light paths shown in Fig. 12, the live animal was under anesthesia, on either a laser scanning confocal microscope or a multiphoton microscope.²⁸ Figure 12(A) shows two series of optical sections obtained by stepping at $12\text{-}\mu\text{m}$ intervals through a primary tumor in a live animal. The left series was obtained with the conventional confocal microscope, and the series on the right was obtained with the multiphoton microscope using a commercial Ti:sapphire laser and an external detector to avoid the confocal pinhole. A comparison of these two z series demonstrates the superiority of the multiphoton microscope in penetrating deep within the live tissue to generate high-resolution confocal images. The greater depth of imaging of the multiphoton microscope compared to the confocal microscope is impressive when one considers that the z series obtained with the multiphoton was started $36\ \mu\text{m}$ inside of the primary tumor and not at the surface, the point at which the signal from

the confocal has fallen away. Hence, while the deepest useful image possible with the conventional confocal was $<40\ \mu\text{m}$, we obtained high-resolution images from depths greater than $300\ \mu\text{m}$ with the multiphoton microscope. In addition, the SNR does not fall off significantly throughout the z series obtained with the multiphoton microscope.

Figure 12(B) shows two series of optical sections identical to those in Fig. 12(A), but repeated to demonstrate the relative amount of bleaching occurring on reexposure of the same optical planes to laser light. The confocal z series on the left is significantly bleached by repeated imaging while the multiphoton z series on the right has a usable SNR at all depths. Therefore, the bleach rate is much less in the multiphoton microscope. In addition, these results demonstrate that, with the imaging conditions used to document cell behavior in this study, bleaching does not affect the interpretation of the images.

This experiment illustrates the advantages of using the multiphoton microscope compared to conventional confocal (and therefore epifluorescence) microscopy in the excitation and emission light paths and therefore the uncaging light path. Excitation and emission of CFP, GFP, and second-harmonic scattered light of 450 nm (from extracellular matrix) is routinely performed with the laser in this light path in whole tissue in live animals with 1- μm z-dimensional resolution. Scan rates of two full fields per second are possible.

7 Conclusion

We described an RNA reporter system and gene-marking technology that could be capable of activating and following RNA synthesis in real time. We also designed and synthesized a light-activatable form of ecdysone and showed its suitability for the light-dependent control of gene expression in cultured cells. Finally, we performed an array of intravital imaging experiments using multiphoton excitation that demonstrates its ability to image deeper and with less phototoxicity versus conventional confocal systems. All of the technologies (caged ecdysteroids, engineering of cells, and multiphoton intravital imaging/illumination) are now in place to assess the feasibility of spatially discrete, light-driven, gene activation in cells and in tissues of whole animals.

Acknowledgment

The authors would like to thank Shailesh Shenoy for his help with the manuscript. This work has been supported by National Institutes of Health (NIH) EB2060, Department of Energy (DOE) ER63056 and P20 EB4930 to Robert H. Singer, NIH R21 GM68993 to David S. Lawrence, CA100324 to John Condeelis.

References

1. E. Bertrand, P. Chartrand, M. Schaefer, S. M. Shenoy, R. H. Singer, and R. M. Long, "Localization of ASH1 mRNA particles in living yeast," *Mol. Cell* **2**, 437–445 (1998).
2. D. Fusco, N. Accornero, B. Lavoie, S. M. Shenoy, J. M. Blanchard, R. H. Singer, and E. Bertrand, "Single mRNA molecules demonstrate probabilistic movement in living mammalian cells," *Curr. Biol.* **13**, 161–167 (2003).
3. S. M. Janicki, T. Tsukamoto, S. E. Salghetti, W. P. Tansey, R. Sachidanandam, K. V. Prasanth, T. Ried, Y. Shav-Tal, E. Bertrand, R. H. Singer, and D. L. Spector, "From silencing to gene expression: Real-time analysis in single cells," *Cell* **116**, 683–698 (2004).
4. Y. Shav-Tal, X. Darzacq, S. M. Shenoy, D. Fusco, S. M. Janicki, D. L. Spector, and R. H. Singer, "Dynamics of single mRNPs in nuclei of living cells," *Science* **304**, 1797–1800 (2004).
5. E. Sahai, J. Wyckoff, U. Philippar, J. E. Segall, F. Gertler, and J. Condeelis, "Simultaneous imaging of GFP, CFP and collagen in tumors in vivo," *BMC Biotech.* (in press).
6. J. Condeelis and J. E. Segall, "Intravital imaging of cell movement in tumours," *Nat. Rev. Cancer* **3**, 921–930 (2003).
7. K. L. Farina, J. B. Wyckoff, J. Rivera, H. Lee, J. E. Segall, J. S. Condeelis, and J. G. Jones, "Cell motility of tumor cells visualized in living intact primary tumors using green fluorescent protein," *Cancer Res.* **58**, 2528–2532 (1998).
8. A. M. Femino, F. S. Fay, K. Fogarty, and R. H. Singer, "Visualization of single RNA transcripts in situ," *Science* **280**, 585–590 (1998).
9. D. No, T. P. Yao, and R. M. Evans, "Ecdysone-inducible gene expression in mammalian cells and transgenic mice," *Proc. Natl. Acad. Sci. U.S.A.* **93**, 3346–3351 (1996).
10. C. Albanese, A. T. Reutens, B. Bouzahzah, M. Fu, M. D'Amico, T. Link, R. Nicholson, R. A. Depinho, and R. G. Pestell, "Sustained mammary gland-directed, ponasterone A-inducible expression in transgenic mice." *FASEB J.* **14**, 877–884 (2000).
11. C. Albanese, J. Hult, T. Sakamaki, and R. G. Pestell, "Recent advances in inducible expression in transgenic mice," *Semin Cell Dev. Biol.* **13**, 129–141 (2002).
12. S. B. Cambridge, R. L. Davis, and J. S. Minden, "Drosophila mitotic domain boundaries as cell fate boundaries," *Science* **277**, 825–828 (1997).
13. F. G. Cruz, J. T. Koh, and K. H. Link, "Light-activated gene expression," *J. Am. Chem. Soc.* **122**, 8777–8787 (2000).
14. W. Lin, C. Albanese, R. G. Pestell, and D. S. Lawrence, "Spatially-discrete light-driven protein expression," *Chem. Biol.* **9**, 1347–1353 (2002).
15. K. Nakanishi, "Ponasterones, compounds with moulting hormone activity," *Bull. Soc. Chim. Fr.* **10**, 3475–3485 (1969).
16. K. Nakanishi, "Past and present studies with ponasterones. The first insect molting hormones from plants," *Steroids* **57**, 649–657 (1992).
17. W. Denk, J. H. Strickler, and W. W. Webb, "Two-photon laser scanning fluorescence microscopy," *Science* **248**, 73–76 (1990).
18. R. M. Williams, W. R. Zipfel, and W. W. Webb, "Multiphoton microscopy in biological research," *Curr. Opin. Chem. Biol.* **5**, 603–608 (2001).
19. D. Kleinfeld, P. P. Mitra, F. Helmchen, and W. Denk, "Fluctuations and stimulus-induced changes in blood flow observed in individual capillaries in layers 2 through 4 of rat neocortex," *Proc. Natl. Acad. Sci. U.S.A.* **95**, 15741–15746 (1998).
20. T. Furuta, S. S. Wang, J. L. Dantzker, T. M. Dore, W. J. Bybee, E. M. Callaway, W. Denk, and R. Y. Tsien, "Brominated 7-hydroxycoumarin-4-ylmethyls: Photolabile protecting groups with biologically useful cross-sections for two photon photolysis," *Proc. Natl. Acad. Sci. U.S.A.* **96**, 1193–1200 (1999).
21. B. Schade, V. Hagen, R. Schmidt, R. Herbrich, E. Krause, T. Eckardt, and J. Bendig, "Deactivation behavior and excited-state properties of (coumarin-4-yl)methyl derivatives. 1. Photocleavage of (7-methoxycoumarin-4-yl)methyl-caged acids with fluorescence enhancement," *J. Org. Chem.* **64**, 9109–9117 (1999).
22. W. Lin and D. S. Lawrence, "A strategy for the construction of caged diols using a photolabile protecting group," *J. Org. Chem.* **67**, 2723–2726 (2002).
23. E. B. Brown, J. B. Shear, S. R. Adams, R. Y. Tsien, and W. W. Webb, "Photolysis of caged calcium in femtoliter volumes using two-photon excitation," *Biophys. J.* **76**, 489–499 (1999).
24. A. F. O'Neill, R. E. Hagar, W. R. Zipfel, M. H. Nathanson, and B. E. Ehrlich, "Regulation of the type III InsP(3) receptor by InsP(3) and calcium," *Biochem. Biophys. Res. Commun.* **294**, 719–725 (2002).
25. W. R. Zipfel, R. M. Williams, and W. W. Webb, "Nonlinear magic: Multiphoton microscopy in the biosciences," *Nat. Biotechnol.* **21**, 1369–1377 (2003).
26. W. Echevarria, M. F. Leite, M. T. Guerra, W. R. Zipfel, and M. H. Nathanson, "Regulation of calcium signals in the nucleus by a nucleoplasmic reticulum," *Nat. Cell Biol.* **5**, 440–446 (2003).
27. C. Minakuchi, Y. Nakagawa, M. Kamimura, and H. Miyagawa, "Binding affinity of nonsteroidal ecdysone agonists against the ecdysone receptor complex determines the strength of their molting hormonal activity," *Eur. J. Biochem.* **270**, 4095–4104 (2003).
28. W. Wang, J. B. Wyckoff, V. C. Frohlich, Y. Oleynikov, S. Huttelmaier, J. Zavadil, L. Cermak, E. P. Bottinger, R. H. Singer, J. G. White, J. E. Segall, and J. S. Condeelis, "Single cell behavior in metastatic primary mammary tumors correlated with gene expression patterns revealed by molecular profiling," *Cancer Res.* **62**, 6278–6288 (2002).
29. J. Wyckoff, J. Segall, and J. Condeelis, in *Single Cell Imaging in Animal Tumors in vivo in Live Cell Imaging: A Laboratory Manual*, D. L. Spector and R. D. Goldman, Eds., Cold Spring Harbor Laboratory Press, Cold Spring Harbor, NY pp. 409–422 (2004).
30. A. Neri, W. D., T. Kawaguchi, and G. L. Nicolson, "Development and biologic properties of malignant cell sublines and clones of a spontaneously metastasizing rat mammary adenocarcinoma," *JNCI, J. Natl. Cancer Inst.* **68**, 507–517 (1982).
31. J. B. Wyckoff, L. Insel, K. Khazaie, R. B. Lichtner, J. S. Condeelis, and J. E. Segall, "Suppression of ruffling by the EGF receptor in chemotactic cells," *Exp. Cell Res.* **242**, 100–109 (1998).